Critical-temperature/Peierls-stress dependent size effects in body centered cubic nanopillars

Seung Min Han, Gang Feng, Joo Young Jung, Hee Joon Jung, James R. Groves et al.

Related Articles

A facile approach to enhance the high temperature stability of magnetite nanoparticles with improved magnetic property
J. Appl. Phys. 113, 044314 (2013)

Thermal conductivity measurement of individual Bi2Se3 nano-ribbon by self-heating three-ω method
Appl. Phys. Lett. 102, 043104 (2013)

Structural and multiferroic properties of Bi1−xInxFeO3 (0≤x≤0.20) nanoparticles
J. Appl. Phys. 113, 044107 (2013)

Surface-enhanced Raman scattering enhancement factor distribution for nanoparticles of arbitrary shapes using surface integral equation method
J. Appl. Phys. 113, 044304 (2013)

Surface enhanced fluorescence and Raman scattering by gold nanoparticle dimers and trimers
J. Appl. Phys. 113, 033102 (2013)

Additional information on Appl. Phys. Lett.

Journal Homepage: http://apl.aip.org/

Journal Information: http://apl.aip.org/about/about_the_journal

Top downloads: http://apl.aip.org/features/most_downloaded

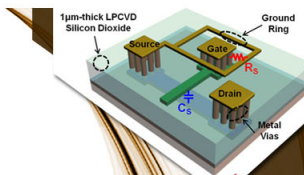Information for Authors: http://apl.aip.org/authors
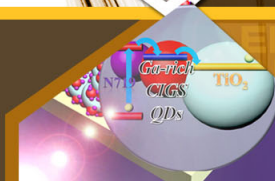
Critical-temperature/Peierls-stress dependent size effects in body centered cubic nanopillars

Seung Min Han,[1,a)] Gang Feng,[2,a)] Joo Young Jung,[1] Hee Joon Jung,[3] James R. Groves,[3] William D. Nix,[3] and Yi Cui[3,a)]

[1]Graduate School of EEWS, Korea Advanced Institute of Science and Technology, Daejeon 305-701, South Korea
[2]Mechanical Engineering, Villanova University, Villanova, Pennsylvania 19085, USA
[3]Department of Materials Science and Engineering, Stanford University, Stanford, California 94305, USA

The size-dependent plasticity of body centered cubic (bcc) metals is different from face centered cubic (fcc) metals: the size-effect exponent n varies for different bcc metal nanopillars ($n = 0.8$–1.0 for V, Nb; $n = 0.3$–0.5 for Ta, Mo, W). This inconsistency is first explained through a simple model based on the temperature-dependent Peierls stress. The bcc V nanopillars with a low critical temperature and Peierls stress showed a fcc-like size effect with $n = 0.79$, and our *in-situ* TEM compression study revealed that fcc-like dislocation starvation occurred in bcc V nanopillars, indicating that a small Peierls stress in V contributes to the fcc-like behavior. © 2013 American Institute of Physics. [http://dx.doi.org/10.1063/1.4776658]

As the size of a metal specimen is decreased to submicron dimensions that are comparable to or smaller than the breeding distance for the dislocations, a strikingly different mechanical behavior arises. In the case of the widely studied single crystalline face centered cubic (fcc) nanopillars,[1–3] the yield strength (σ_y) is known to increase with a decrease in diameter (d) according to $\sigma_y \propto d^{-n}$, where the size-effect exponent n for fcc metals mostly falls in the range of 0.6 to 1.0.[4,5] In addition, discrete plasticity with frequent strain bursts become more pronounced as the size of the nanopillar is reduced. Although there is agreement with the reported size dependent mechanical behavior, there is debate as to whether the deformation mechanism is due to the dislocation starvation as proposed by Greer and Nix[2] or due to the activation of a single-armed source as proposed by Parthasarathy *et al.*[6] In both the dislocation starvation and the single-armed source theories, understanding the dislocation multiplication process in the nanopillar can provide insights to the responsible deformation mechanism. Therefore, studying the size dependent mechanical behavior in other types of crystalline structures with intrinsically different dislocation motion is of interest.

Among the common crystal structures found in metals, body centered cubic (bcc) metals pose different conditions for plasticity compared with the fcc metals, because of the higher Peierls stress and easier cross-slip for the slower screw dislocations. The dislocations in bcc metals are known to move more sluggishly in the crystalline lattice due to the Peierls stress (lattice friction), and the addition of the cross-slip mechanism will increase the probability of forming dislocation networks, leading to the creation of immobile dislocation sources inside the nanopillar. In the molecular dynamics simulation study by Weinberger and Cai,[7] a Mo bcc nanopillar was shown to result in "surface-aided multiplication," where the cusp formation occurs in a single dislocation that starts to glide on two different slip planes of {110} and {112} that eventually leads to self-multiplication of the dislocation. Weinberger and Cai[7] also noted that the critical stress needed for self-multiplication is higher for smaller pillar diameters. Therefore, the governing deformation mechanism for bcc nanopillars may be different from that of fcc nanopillars, and a systematic study of bcc nanopillars will give insights to the responsible deformation mechanisms under different dislocation multiplication conditions.

Recently, there have been several experimental studies on the size dependent properties of bcc metals,[8–15] including our previous report on vanadium *ex-situ* nanopillar compression testing.[15] The pillar compression studies of different bcc metals including V, Nb, Ta, Mo, and W have been reported,[8–14] and the results indicate that the degree of size dependency varies for different bcc metals. For example, Mo nanopillars showed a size effect exponent n ranging from 0.3 to 0.5,[8–10,13] which is significantly lower than the commonly observed n for fcc metals, which is in the range of 0.6 to 1.0.[4,5] On the other hand, the V nanopillars showed $n = 0.79$,[15] which is within the commonly observed value for fcc metals. Thus, different bcc metals were shown to display different size effects,[8–14] and a postulated cause is the difference in the ratio of the pillar-testing temperature to a critical temperature (T_c).[16,17] Generally, for bcc metals, when the testing temperature is at or above the critical temperature (T_c) at which the thermal activation occurs over the Peierls barrier, the screw dislocations would glide much easier or the Peierls stress for bcc metals becomes effectively very small.[18] The above mentioned pillar compression studies were all conducted at room temperature,[8–14] and different bcc metals would have different Peierls stresses. Bulk vanadium has a relatively low critical temperature which is in the range of 200 K–380 K based on different studies.[19–21] Therefore, the testing temperature of 298 K in our previous study on V nanopillars might be very close to the critical temperature for the V nanopillars,[15] so that the Peierls stress in these

a)Authors to whom correspondence should be addressed. Electronic addresses: smhan01@kaist.ac.kr, gang.feng@villanova.edu, and yicui@stanford.edu.
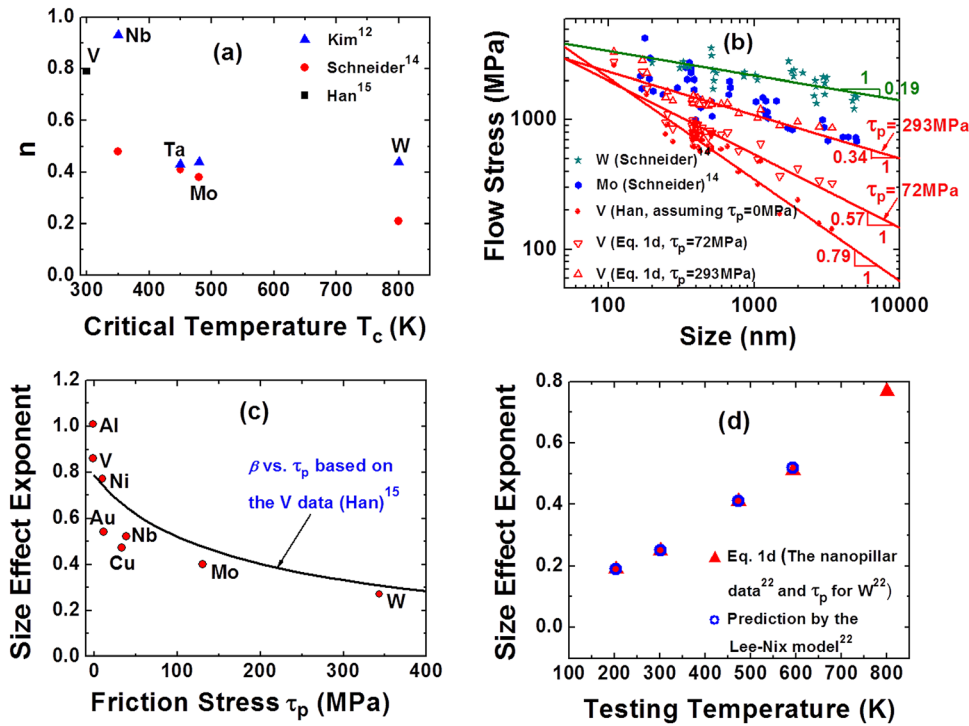
FIG. 1. (a) Size exponent n vs. the respective critical temperatures for V taken from the work by Han *et al.* (see Ref. 15) and Nb, Ta, Mo, W taken from the work of Kim *et al.* (see Ref. 12) and Schneider *et al.* (see Ref. 14). (b) Pillar flow stress vs. pillar size for W, Mo, and V, where, the V data (solid circles) are taken from the work by Han *et al.* (see Ref. 15), and the W and Mo data are taken from Schneider *et al.* (see Ref. 14). Moreover, two data sets for V are also shown and calculated through Eq. (1d) based on the V data (solid circles) and the corresponding τ_p input. (c) The experimental size-effect exponent vs. the Peierls stress which is taken from the work of Lee and Nix (see Ref. 22). The black solid line represents the prediction by fitting the data calculated through Eq. (1d) based on the V data (solid red circles in (b)) and the corresponding τ_p input. (d) The calculated size effect exponent vs. the testing temperature for W pillars. Here, the blue hollow circle represents the data extracted from the work of Lee and Nix (see Ref. 22), while the red solid triangle data are calculated by the following steps: (i) extract the flow stress vs. pillar size data at 28 °C from the Fig. 8 in the work of Lee and Nix (see Refs. 5, 22, and 24); (ii) calculate σ_o vs. the pillar size (d) through Eq. (1d) based on the data extracted in step (i) and the corresponding $\tau_p = 294$ MPa; (iii) for each of the other testing temperatures, calculate σ_y vs. d through Eq. (1d) based on the σ_o obtained in step (ii) and the corresponding τ_p, and then the plot of σ_y vs. d can be fitted to determine the corresponding size-effect exponent.

V nanopillars would be small, making them behave like fcc metals. Thus, our previous report on V size dependent plasticity[15] attributed the similarity in size effect exponent n between V and fcc metals to the potential removal of dislocations that results in dislocation starvation as opposed to dislocation accumulation through the multiplication process as observed in Mo, W, and Ta nanopillars.[15]

The above mentioned critical-temperature dependent size-effect exponent n can be clearly shown in a plot of n vs. the respective critical temperatures T_c for different bcc metals as in Fig. 1(a), and this is plotted based on the studies by Kim *et al.*,[12] Schneider *et al.*,[14] and Han *et al.*[15] W, Mo, and Ta have $T_c > 450$ K, and therefore, the thermal energy at the testing temperature (~300 K) is not enough for thermal activation over the Peierls barrier, which results in a higher lattice friction for dislocation motion and a correspondingly small size effect exponent of $n < 0.5$. However, Fig. 1(a) indicates a steep rise in n for V and Nb nanopillars, where the critical temperatures are close to the room temperature testing conditions: V has T_c of 200 K–380 K (Refs. 19–21) and Nb has T_c of 350 K.[14] Therefore, the thermal energy at the testing temperature (~300 K) may be enough to provide thermal activation over the Peierls barrier for V and Nb that results in a fcc-like size effect behavior (dislocation starvation and $n = 0.8$–1.0) due to a very small effective Peierls stress.

This critical-temperature dependency of the size-effect exponent n as shown in Fig. 1(a) may be further qualitatively understood by the following simple model. The yielding stress σ_y of pillar compression testing has been commonly fitted in a power law form as

$$\sigma_y = Ad^{-n}, \tag{1a}$$

where A is a constant and n is the size-effect exponent as discussed above. It is known that the strengthening factors that contribute to the prediction in yield stress including lattice friction and dislocation elastic interaction, are generally additive.[22] Consequently, the yielding stress of a nanopillar can be expressed by

$$\sigma_y = \frac{\tau_p}{m} + \sigma_o, \tag{1b}$$

where τ_p is the Peierls stress, which is generally not dependent on the pillar size d, m is the Schmid factor, and σ_o is the yielding strength due to all other strengthening factors except the Peierls lattice friction, such as the activation stress for dislocation sources, and the stress associated with dislocation interactions.[22] As discussed above, the Peierls stress τ_p for Nb and V nanopillars may be very small, so that we may expect a size effect behavior similar to that of fcc metals, i.e., $\sigma_o \approx \sigma_y = Ad^{-n}$, with an n in the range of 0.6–1.0. On

the other hand, the Peierls stress τ_p for Mo, Ta, and W nanopillars at room temperature may be quite large, and at the same time, as a first order estimation, we can assume that all other strengthening factors for bcc nanopillars operate similarly, i.e., $\sigma_o \approx Ad^{-n}$ with n in the range of 0.6–1.0 as for V and Nb nanopillars. Thus, based on Eq. (1b), for Mo, Ta, and W nanopillars, we have

$$\sigma_y = \frac{\tau_p}{m} + Ad^{-n} \quad \text{with} \quad 0.6 < n < 1.0. \qquad (1c)$$

However, for pillar compression testing of Mo, Ta, and W, as is common practice, we would force the results to be fitted in the form of Eq. (1a), i.e.,

$$\sigma_y = \frac{\tau_p}{m} + Ad^{-n} = Bd^{-\beta} \quad \text{with} \quad 0.6 < n < 1.0, \qquad (1d)$$

where B is a fitting constant, and β is the fictitious size-effect exponent from curve fitting. Mathematically, β is always smaller than n as shown in Fig. 1(b). If we perform pillar compression testing at a temperature much lower than T_c, the Peierls stress τ_p may not be negligible and could be as high as 800 MPa for bcc metals.[18,23] Therefore, based on Eq. (1d), we will expect a smaller size-effect exponent β for Mo, Ta, and W.

To have a quantitative demonstration, the experimental pillar compression data for [001] V nanopillars[15] in Fig. 1(b) can be analyzed. The original data show $n = 0.79$ for which we can assume $\tau_p \approx 0$. If $\tau_p = 72$ MPa, and noticing that the Schmid factor is $m = 1/\sqrt{6}$, then the effective yielding stress can be estimated by adding $72\sqrt{6}$ MPa to each data point; thus, the fictitious size-effect exponent $\beta = 0.57$ as in Fig. 1(b). If $\tau_p = 293$ MPa, $\beta = 0.34$ as in Fig. 1(b) after a similar analysis. It is interesting to see that the resulting data by choosing $\tau_p = 293$ MPa for V nanopillars match the experimental results of the Mo nanopillars. Similarly, based on the same data for V nanopillars, we can get a plot of β vs. τ_p (see Fig. 1(c)) which matches the experimentally determined n vs. τ_p relation surprisingly well.

Furthermore, if we know the temperature dependence of τ_p as well as the relation between σ_y and d at one temperature, then, based on Eq. (1d), we can easily estimate the relation of the size-effect exponent vs. the testing temperature. For example, for W, $\tau_p = 447$ MPa, 294 MPa, 119 MPa, and 66 MPa at $T = -77\,^\circ$C, $28\,^\circ$C, $200\,^\circ$C, and $320\,^\circ$C, respectively;[22] at the critical temperature ($527\,^\circ$C) of W, τ_p can be assumed to be 0 MPa. Fig. 1(d) compares the prediction by Eq. (1d) for W nanopillars and the prediction based on a much more elaborate model by Lee and Nix[22] in which the Peierls stress effect is also considered, indicating a very good match between our simple model (Eq. (1d)) and the Lee-Nix model.[22]

In order to confirm that the difference in experimental n for bcc metals at room temperature is due to different dislocation behavior arising from different T_c and thus different τ_p, we used *in-situ* TEM nanopillar compression to investigate the V single crystal nanopillars, and we confirmed that the dislocation behavior in V nanopillars at room temperature is indeed fcc-like, i.e., running out the nanopillars quickly and reaching a dislocation starvation state. Among

different choices of bcc metals previous studied for size effects,[10–13] V has a small atomic number, making V well-suited for *in-situ* TEM observation to provide evidence for the deformation mechanism.

An *in-situ* TEM nanopillar compression study of V, however, requires careful design of the specimen to synthesize electron transparent single crystalline V nanopillars with non-obstructed views for imaging. We have deposited an epitaxial V film on top of a (001) Si wafer with a thin wedge structure that is $1\,\mu$m in width by utilizing a textured MgO seed layer. First, the (001) Si wedge structure, commercially available from Hysitron, is created by lithographically etching (001) Si to leave a $1\,\mu$m width wedge for non-obstructed viewing inside the TEM. In order to grow epitaxial V on top of this Si wedge structure, a textured MgO seed layer was deposited using the ion beam assisted deposition (IBAD) process.[25] The resulting MgO layer is a polycrystalline layer with (001) texture that is 17 nm in thickness. Following the IBAD MgO layer deposition, the V could then be grown epitaxially by e-beam evaporation at $600\,^\circ$C. The thin V wedge with a total of $1\,\mu$m in width is then etched into nanopillars with diameter of ~200 nm using the focused ion beam (FIB). The schematic of our V nanopillar TEM specimen design and the TEM micrograph of a representative V nanopillar are shown in Fig. 2. Selected area diffraction (SAD) of the nanopillar confirmed that the V is single crystal within the pillar that has (001) out-of-plane orientation as we had intended.

The V nanopillars were tested *in-situ* in compression using a Hysitron Picoindenter (PI-95) in a FEI Tecnai G2 F20. The nanopillars were compressed at a nominal constant displacement rate of 2 nm/s, and the resulting true stress vs. true strain plot calculated using the constant volume, homogeneous deformation model is shown in Fig. 3(e). The average flow stresses at 2% plastic strain were determined to be 1.13 GPa and 1.17 GPa for the two pillars shown in Figs. 3(a) and 3(b) with diameters of 147 nm and 169 nm, and this is comparable to the previous *ex-situ* values of 1.1 GPa for V nanopillars of ~200 nm in diameter.[15] After confirming that the *in-situ* testing of V nanopillars was displaying similar stress vs. strain behavior as in the *ex-situ* testing,[15] the TEM images were analyzed to check dislocation activities. The TEM micrographs before and after deformation are shown in Figs. 3(a)–3(d), and the *in-situ* TEM compression is shown in the movie linked in Fig. 3. A significant reduction in the dislocation density within the deformed volume at the top of the nanopillar is apparent when comparing the before and the after deformation micrographs. In the case of *in-situ* TEM testing of Ni nanopillars by Shan et al.,[26] the dislocations were quickly removed from the body of the pillar during deformation, leaving the pillar essentially defect free. However, in the case of vanadium, some dislocations were still present within the nanopillar although there is a significant reduction in the density after compression. Therefore, we observe that the dislocations do not result in multiplications but leave the V nanopillar during deformation, but at a slower reduction rate than that observed for Ni nanopillars. This slower dislocation-removal rate is as expected for V since the glide motion in bcc metals is intrinsically more difficult where slip occurs on {110} or
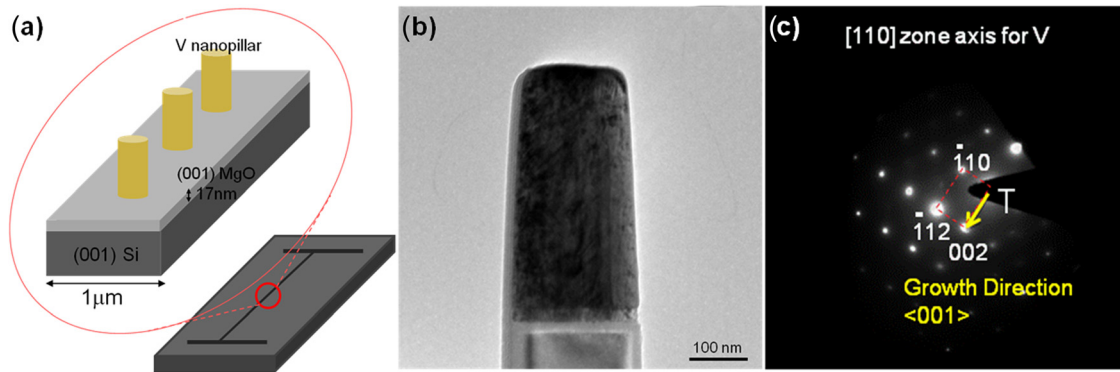
FIG. 2. (a) Epitaxial V film was grown on top of (001) MgO on Si wedge that is 1 μm in width and nanopillars were then etched using focused ion beam. (b) TEM image and (c) SAD confirming that the V pillar is single crystal with [001] orientation.

{112} planes instead of the close packed {111} planes in fcc. Therefore, although the critical temperature is close to the testing room temperature condition, V is retaining slightly more dislocations within the lattice compared to the
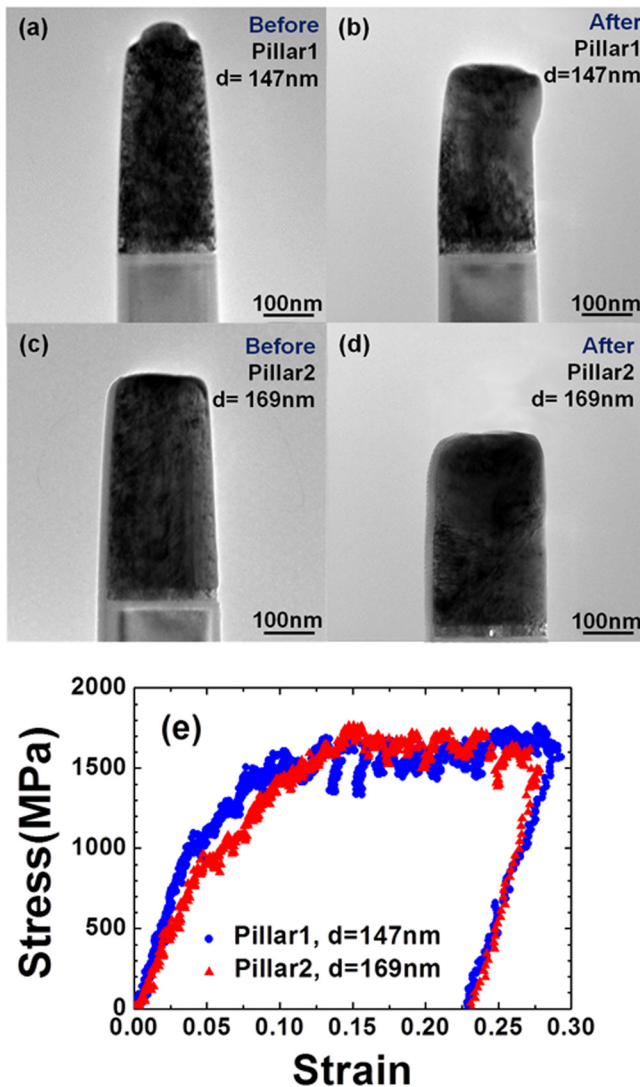

FIG. 3. TEM images of (a), (c) before and (b), (d) after compression testing of two V nanopillars (e) the resulting true stress vs. true strain plots. Flow stresses at 2% plastic strain were determined to be 1.13 GPa for d = 147 nm and 1.17 GPa for d = 169 nm pillars (enhanced online) [URL: http://dx.doi.org/10.1063/1.4776658.1].

case of fcc metals. Thus, at room temperature, τ_p for V is not negligible as for fcc metals but still very small.

The deformed nanopillars were analyzed further using SAD as in Figs. 4(a) and 4(b) that revealed a grain rotation in the deformed region from the original [001] to [-1-12] along the compression axis. If a [001] perfectly oriented nanopillar is uniformly deformed under uniaxial compression, we may expect a homogeneous deformation with multiple slip systems activated (equal slip operations on (101), (011), (0-11), and (-101) planes), and hence grain rotation should not occur. However, it is common that the compression axis may be slightly misoriented compared to the [001] orientation of the single crystal nanopillars, and also that one slip system may dominate due to the stochastic nature of plastic flow, and that can result in grain rotation.

The evolution of the aforementioned grain rotation from [001] to [-1-12] can be understood as follows. For uniaxial testing of V single crystals, the slip direction is ⟨111⟩, but the slip plane is less certain and could be {110},[27,28] {112}[20,29] or mixture of these depending on the testing temperature,[20,21,27,29] loading direction,[20,30] and impurity concentration.[29] The slip involving *both* {110} and {112} is called ⟨111⟩-pencil glide,[31] and [001] is a stable end-orientation under ⟨111⟩-pencil glide if the compression axis is within ∼10° of [001].[31,32] Also, if {112} is the *sole* active slip plane, the [001] is also a stable end-orientation under compression.[30,33] Thus, for compression along [001], the slip involving *both* {110} and {112} and that involving *solely* {112} would result in no crystal rotation, which is not consistent with our result of [112] along the loading axis after compression.

Therefore, the slip plane for our V nanopillars should be {110}, which turns out to be consistent with the crystal rotation from [001] to [-1-12] as follows (see Fig. 4(c)). It is known that the slip plane normal will rotate towards the compression axis under compression.[30,31] Suppose that, due to a small misorientation as discussed before, the original compression axis is along a direction shown in Fig. 4(c), and the primary slip system according to the Diehl rule[30] would be (011)[1-11]. Thus, during compression, the compression axis will rotate along a great circle towards the (011) pole, and the rotation will normally "overshoot"[30] into the neighboring 001-011-111 unit triangle in which the slip system becomes (101)[-111]. Then, the compression axis will rotate along a great circle towards the (101) pole and then
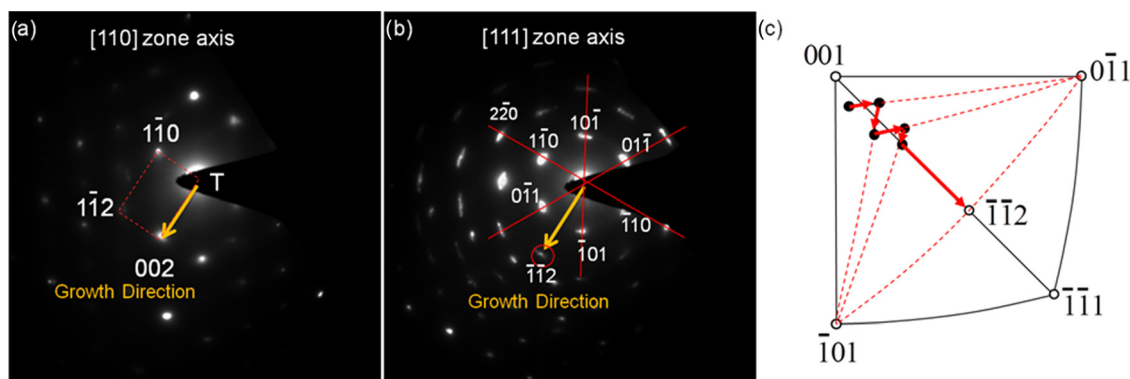
FIG. 4. The SADs (a) at the bottom of the pillar and (b) in the deformed area, indicating grain rotation in the deformed region from [001] to [-1-12] along the compression axis. (c) Stereogram indicating the pathway for grain rotation, where the red dash lines indicate the great circles.

"overshoot." After the multiple transitions of the compression axis between the two 001-011-111 unit triangles as shown in Fig. 4(c), the stable end orientation would be [-1-12], as [011], [112], and [101] are along a great circle. These multiple transitions could be also achieved as the simultaneous activation of the two slip systems: (011)[1-11] and (101)[-111]. Thus: (1) the slip plane for V-nanopillar is solely {110}, and (2) the stochastic flow behavior in single crystalline metals may cause grain rotations from unstable end-orientation that may be otherwise kept with uniform activation of multiple slip systems.

In summary, it is argued that the size effects on the strength of bcc nanopillars are dependent on the critical temperature (T_c) and, equivalently, the Peierls stress (τ_p). When the testing temperature (T) is higher than the T_c for a bcc metal, τ_p can be neglected, and the strengthening mechanism is similar to that for fcc metals with the size-effect exponent n in the range of 0.8–1.0. When $T < T_c$, the effect of τ_p cannot be neglected, and based on a simple model (Eq. (1d)), n would decrease with increasing τ_p. Thus, when tested at room temperature, Nb and V nanopillars with T_c close to 300 K show a high n (similar to fcc metals), and Mo, Ta, and W nanopillars with $T_c \gg 300$ K show much lower n. The *in-situ* TEM compression on V nanopillars showed a clear reduction in the dislocation density after deformation, suggesting a low τ_p for V at room temperature, as expected. Thus, even though V is a bcc metal, it displayed a loss of dislocation content due to its low T_c and low τ_p that facilitated dislocation motion and easier removal from the body of the nanopillar, although the rate of removal is slightly slower than that for fcc nanopillars. The *in-situ* TEM also indicated that the slip plane for the V-nanopillar is solely {110} (not {112}), and that the stochastic flow behavior in single crystalline metals may cause grain rotations from unstable end-orientation that may be otherwise avoided with uniform activation of multiple slip systems.

[1]M. D. Uchic, D. M. Dimiduk, J. N. Florando, and W. D. Nix, Science **305**(5686), 986 (2004).
[2]J. R. Greer, W. C. Oliver, and W. D. Nix, Acta Mater. **53**(6), 1821 (2005).
[3]C. A. Volkert and E. T. Lilleodden, Philos. Mag. **86**(33–35), 5567 (2006).
[4]M. D. Uchic, P. A. Shade, and D. M. Dimiduk, Annu. Rev. Mater. Res. **39**, 361 (2009).
[5]J. R. Greer and J. T. M. De Hosson, Prog. Mater. Sci. **56**(6), 654 (2011).
[6]T. A. Parthasarathy, S. I. Rao, D. M. Dimiduk, M. D. Uchic, and D. R. Trinkle, Scr. Mater. **56**(4), 313 (2007).
[7]C. R. Weinberger and W. Cai, Proc. Natl. Acad. Sci. U.S.A. **105**(38), 14304 (2008).
[8]J. R. Greer, C. R. Weinberger, and W. Cai, Mater. Sci. Eng., A **493**(1–2), 21 (2008).
[9]J. Y. Kim and J. R. Greer, Appl. Phys. Lett. **93**(10), 101916 (2008).
[10]J. Y. Kim and J. R. Greer, Acta Mater. **57**(17), 5245 (2009).
[11]J. Y. Kim, D. C. Jang, and J. R. Greer, Scr. Mater. **61**(3), 300 (2009).
[12]J. Y. Kim, D. C. Jong, and J. R. Greer, Acta Mater. **58**(7), 2355 (2010).
[13]A. S. Schneider, B. G. Clark, C. P. Frick, P. A. Gruber, and E. Arzt, Mater. Sci. Eng., A **508**(1–2), 241 (2009).
[14]A. S. Schneider, D. Kaufmann, B. G. Clark, C. P. Frick, P. A. Gruber, R. Monig, O. Kraft, and E. Arzt, Phys. Rev. Lett. **103**(10), 105501 (2009).
[15]S. M. Han, T. Bozorg-Grayeli, J. R. Groyes, and W. D. Nix, Scr. Mater. **63**(12), 1153 (2010).
[16]T. Suzuki, H. Koizumi, and H. O. K. Kirchner, Acta Metall. Mater. **43**(6), 2177 (1995).
[17]A. Seeger and U. Holzwarth, Philos. Mag. **86**(25–26), 3861 (2006).
[18]D. E. Segall, A. Strachan, W. A. Goddard, S. Ismail-Beigi, and T. A. Arias, Phys. Rev. B **68**(1), 014104 (2003).
[19]B. C. Masters and J. W. Christian, Proc. R. Soc. London, Ser. A **281**, 240 (1964).
[20]C. T. Wang and D. W. Bainbridge, Metall. Mater. Trans. B **3**(12), 3161 (1972).
[21]H. Conrad and W. Hayes, Trans. Am. Soc. Met. **56**, 125 (1963).
[22]S. W. Lee and W. D. Nix, Philos. Mag. **92**(10), 1238 (2012).
[23]K. G. Hoge and A. K. Mukherjee, J. Mater. Sci. **12**(8), 1666 (1977).
[24]W. D. Nix and S. W. Lee, Philos. Mag. **91**(7–9), 1084 (2011).
[25]S. Gsell, M. Schreck, R. Brescia, B. Stritzker, P. N. Arendt, and J. R. Groves, Jpn. J. Appl. Phys., Part 1 **47**(12), 8925 (2008).
[26]Z. W. Shan, R. K. Mishra, S. A. S. Asif, O. L. Warren, and A. M. Minor, Nature Mater. **7**(2), 115 (2008).
[27]T. E. Mitchell, R. J. Fields, and R. L. Smialek, J. Less-Common Met. **20**(2), 167 (1970).
[28]J. Bressers and P. De Meester, J. Less-Common Met. **84**, 11 (1982).
[29]E. S. Greiner and D. M. Boulin, Trans. Metall. Soc. AIME **239**(7), 965 (1967).
[30]A. Kelly and K. M. Knowles, *Crystallography and Crystal Defects*, 2nd Edition (Wiley, Malden, MA, 2012).
[31]W. F. Hosford, *Mechanical Behavior of Materials* (Cambridge University Press, New York, 2005).
[32]J. M. Rosenberg and H. R. Piehler, Metall. Mater. Trans. B **2**(1), 257 (1971).
[33]C. J. Hamelin, "Multi-Scale Modelling of Texture Evolution and Surface Roughening of BCC Metals During Sheet Forming, Type, Mechanical and Materials Engineering," Thesis, Queen's University (2009).